Search for tetrahedral states in Yb nuclei with N~90 through Coulomb excitation using HIE-ISOLDE and Miniball

C.M. Petrache – University Paris-Sud & CSNSM Orsay

- ISOLDE, CERN
- Strasbourg, France
- Darmstadt, Germany
- Köln, Germany
- Athens, Greece
- Maryland, USA
- Kolkata, India

ISOLDE RILIS Yields of Yb nuclei

6. Ytterbium

Yb was the first element tested off- and on-line at the ISOLDE RILIS [1]. Neutron-deficient Yb isotopes down to ^{153}Yb were ionized and used for in-source atomic spectroscopy with the RILIS of the IRIS facility in Gatchina [24]. Here we report the yields obtained at ISOLDE with a standard Ta foil target and W ionizer. [5] With the RILIS the Yb yields were enhanced by a factor of about 20 against surface ionization. The now measured on-line efficiency was probably below the off-line measured 15% [1]. Note that the W ionizer is

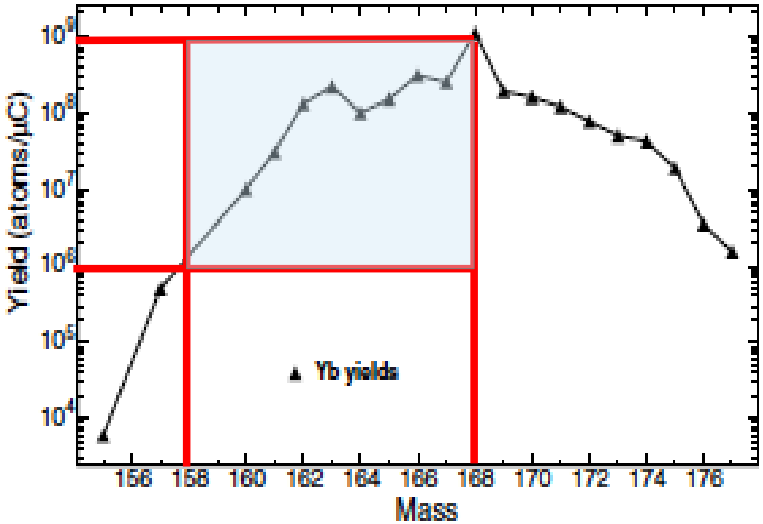

Fig. 3. Ion yields of ytterbium isotopes from a Ta foil target.

Group point symmetries are present in nuclei ?

- Group theory provides a powerful means of classifying spectra in terms of group representations.
- The irreducible representations determine the degeneracies of spectra and thus the underlying shell structure.
- Fermion mean-field Hamiltonians are described with double point groups, out of which only three – tetrahedral (pyramid) T_d, octahedral (diamond) O_h and icosahedral I_h lead to exotic 4-fold degeneracies of single Fermion levels.
- This high degeneracy leads to large gaps (magic numbers) and high stability of the nuclear shape.
- Invariant surfaces can be modeled selecting appropriately a subset of spherical harmonics that are allowed by a given symmetry.

J. Dudek et al., PRL 97 (2006)

Octahedral and thetrahedral shapes

$$\mathcal{R}(\vartheta,\varphi;\hat{\alpha}) = R_0\, c(\hat{\alpha})\left[1+\sum_{\lambda=2}^{\lambda_{\max}}\sum_{\mu=-\lambda}^{\lambda}\alpha_{\lambda,\mu}\, Y_{\lambda,\mu}(\vartheta,\varphi)\right]$$

$$\hat{\alpha} \equiv \{\alpha_{\lambda,\mu};\ \lambda = 2,3,\ \ldots\lambda_{\max};\ \mu = -\lambda,\ -\lambda+1,\ldots\ +\lambda\}$$

$\alpha_{40} \equiv +o_1;\quad \alpha_{4,\pm4} \equiv +\sqrt{\frac{5}{14}}\,o_1;\quad \alpha_{60} \equiv +o_2;\quad \alpha_{6,\pm4} \equiv -\sqrt{\frac{7}{2}}\,o_2$

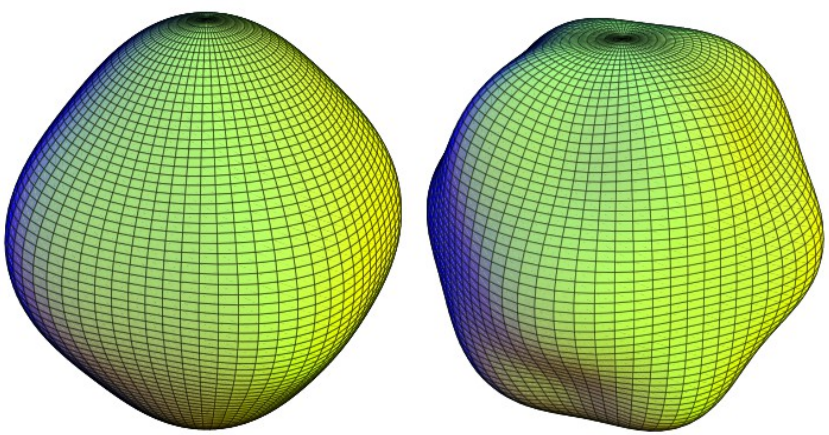

Fig. 1. Comparison of two octahedrally deformed nuclei. Left: octahedral deformation of the first order, $o_1 = 0.10$; right: octahedral deformation of the second order, $o_2 = 0.04$.

$\alpha_{3,\pm2} \equiv t_1 \qquad \alpha_{7,\pm2} \equiv t_2\,; \qquad \alpha_{7,\pm6} \equiv -\sqrt{\frac{11}{13}}\,t_2$

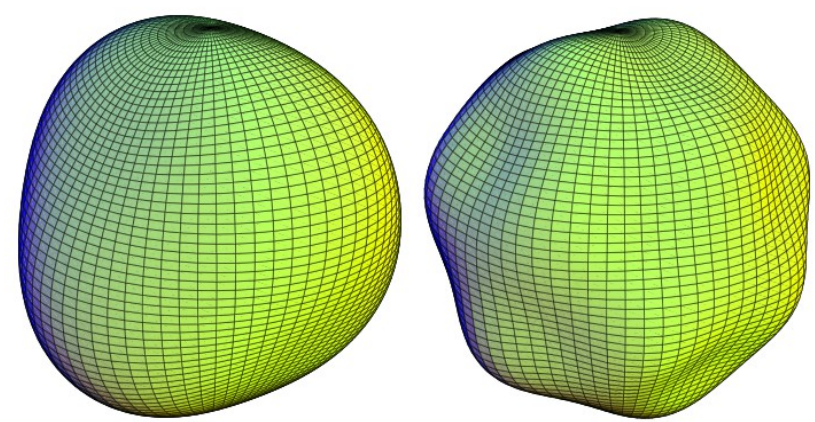

Fig. 2. Comparison of two tetrahedrally deformed nuclei. Left: tetrahedral deformation of the first order, $t_1 = 0.15$; right: tetrahedral deformation of the second order, $t_2 = 0.05$.

Tetrahedral symmetric surfaces at increasing values of rank λ deformations α_{32} = 0.1, 0.2, 0.3

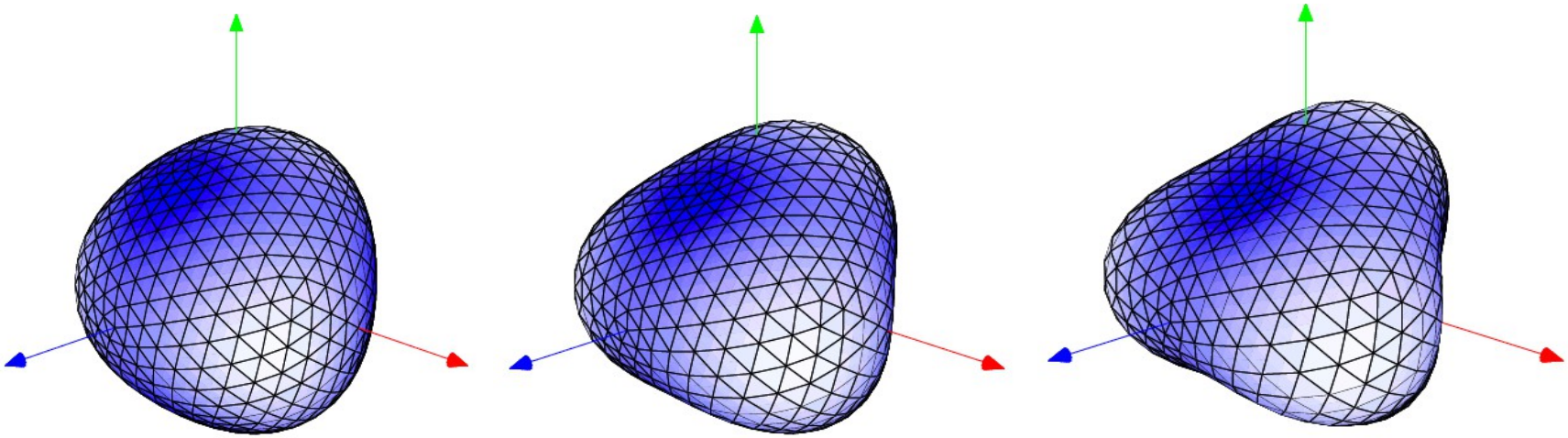

Octahedral and thetrahedral spectra

Octahedral

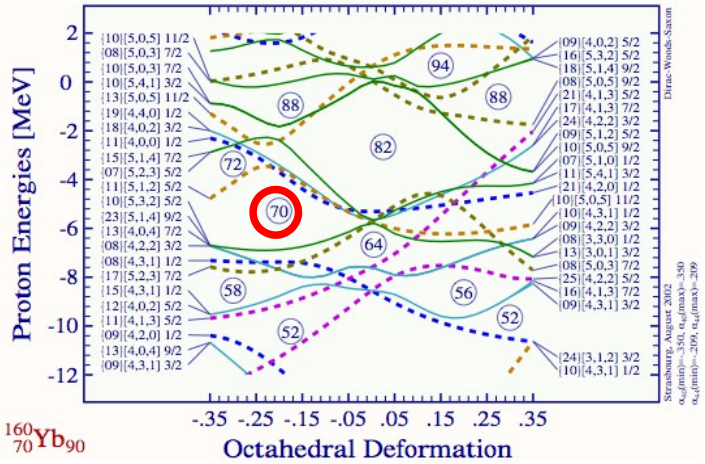

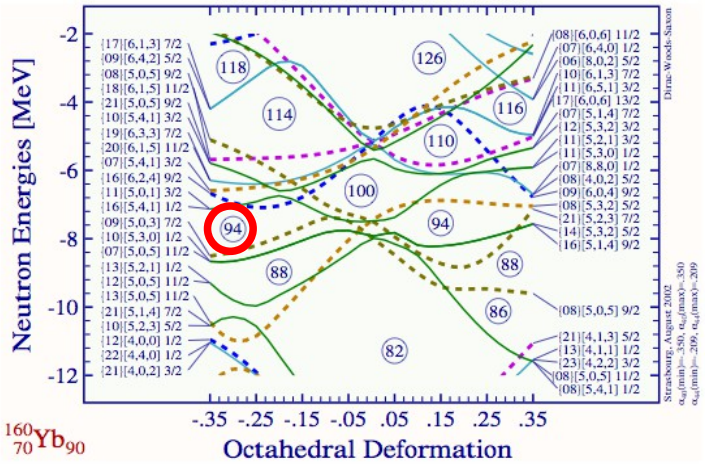

Tetrahedral

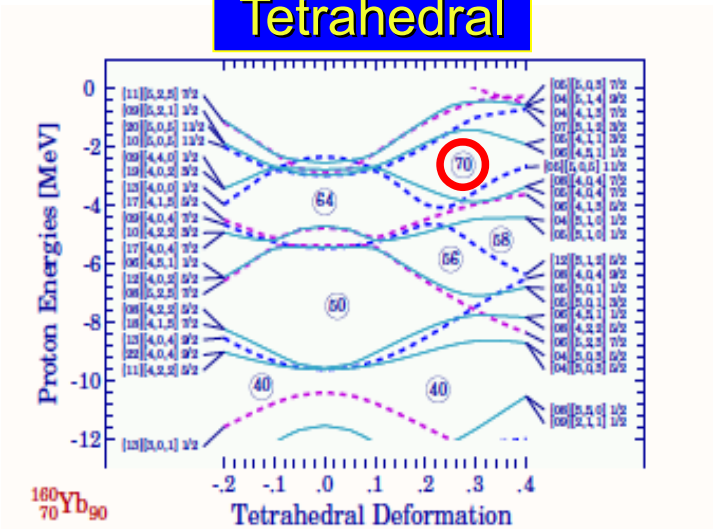

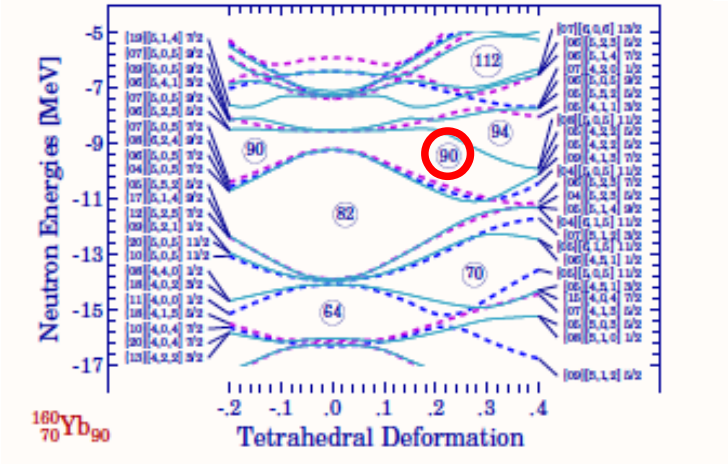

4-fold degeneracies => new large (magic) gaps

Nuclear Tetrahedral Symmetry: Possibly Present throughout the Periodic Table

J. Dudek,[1] A. Goźdź,[1,2] N. Schunck,[1] and M. Miśkiewicz[2]

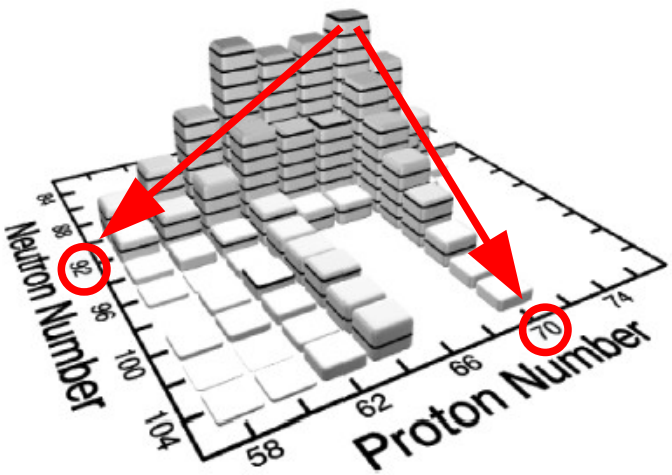

FIG. 3. Barriers between tetrahedral and quadrupole minima (cf. Fig. 1 bottom). Each brick in the stack represents 100 keV.

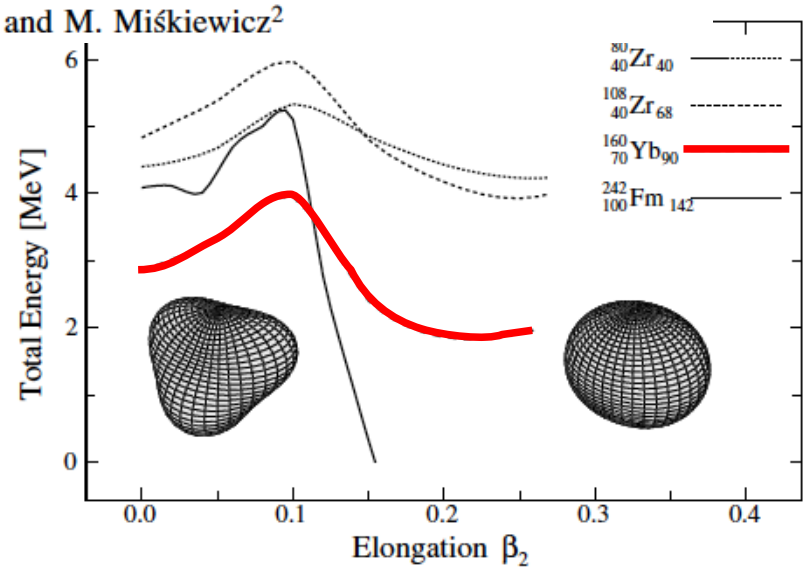

FIG. 2. Results of the multidimensional minimization of the total nuclear energies projected on the quadrupole deformation axis. The gamma deformation as well as all other deformations vary along the β_2 axis following the minimization, for each curve separately. The left-hand side inset shows an exaggerated (for better visibility) view of the tetrahedral shape at $\alpha_{32} = 0.3$, roughly twice the calculated equilibrium deformation. The right-hand side inset shows for comparison an oblate shape surface at $\beta_2 = 0.20, \gamma = 60^0$, i.e., roughly at the calculated equilibria.

lows: The strongest tetrahedral-symmetry effects appear at proton numbers $Z_t = 16, 20, 32, 40, 56–58^*, 70^*$, and $90–94^*$, where the asterisks denote the gaps that are particularly strong (up to ~3 MeV or so). A clear proton-neutron symmetry exists in the calculations leading to the related tetrahedral neutron gaps at $N_t = 16, 20, 32, 40, 56–58^*, 70^*, 90–94^*, 112$, and $136/142$.

Desexcitation patterns

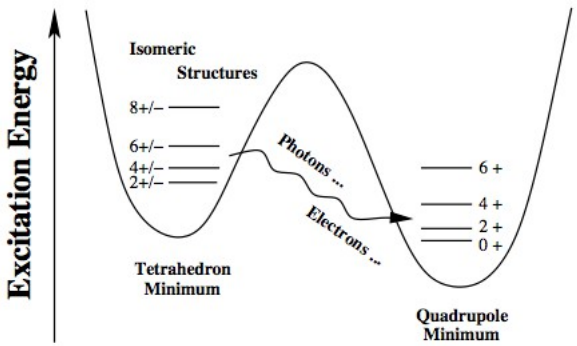

Fig. 7. Schematic illustration: structure and possibilities of the decay out of a tetrahedral minimum. Since the lowest-order tetrahedral deformation has the same geometrical features as the octupole deformation α_{32}, the concerned nuclei may generate parity-doublet rotational bands known from the studies of the octupole shapes. Establishing the structure of the bands (parity doublets?), the nature of the inter- and intra-band transitions (dipole? quadrupole? octupole?), the properties of the side-feeding and the decay branching ratios all that will greatly help identifying the symmetry through experiments.

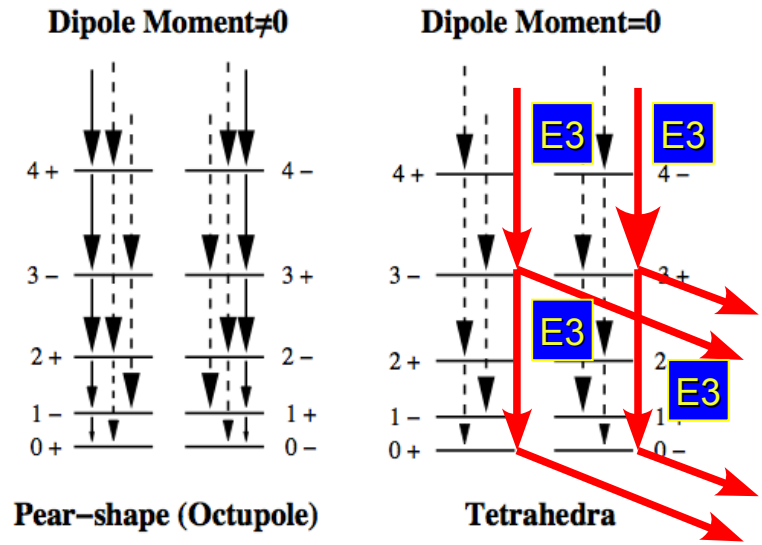

PRL 97, 072501 (2006) PHYSICAL REVIEW LETTERS week ending 18 AUGUST 2006

Island of Rare Earth Nuclei with Tetrahedral and Octahedral Symmetries: Possible Experimental Evidence

J. Dudek,[1] D. Curien,[2] N. Dubray,[1] J. Dobaczewski,[3] V. Pangon,[1] P. Olbratowski,[3] and N. Schunck[4]

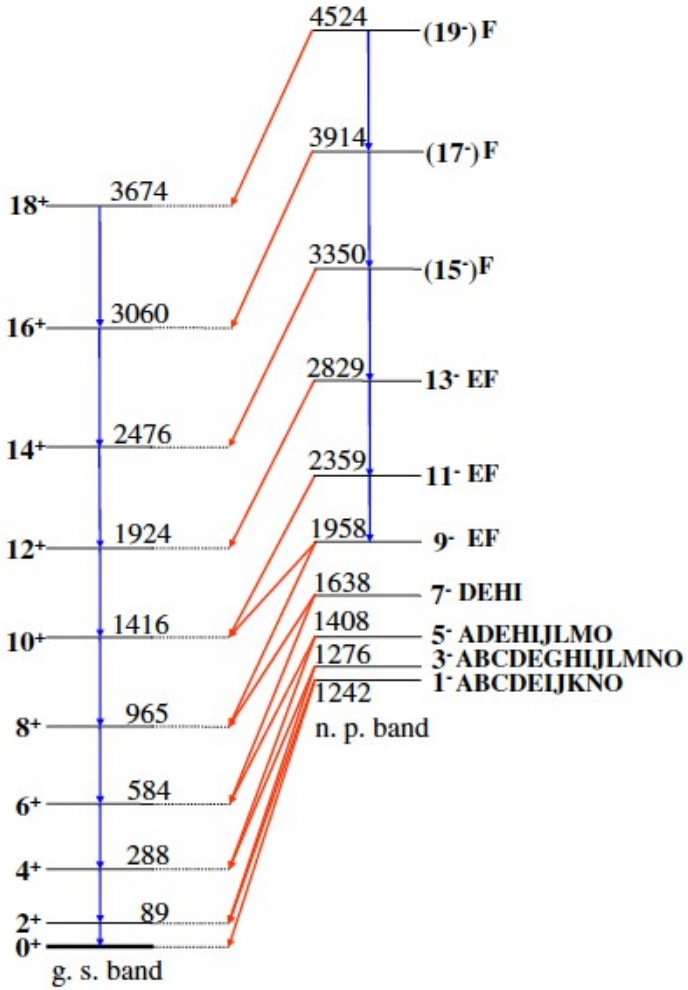

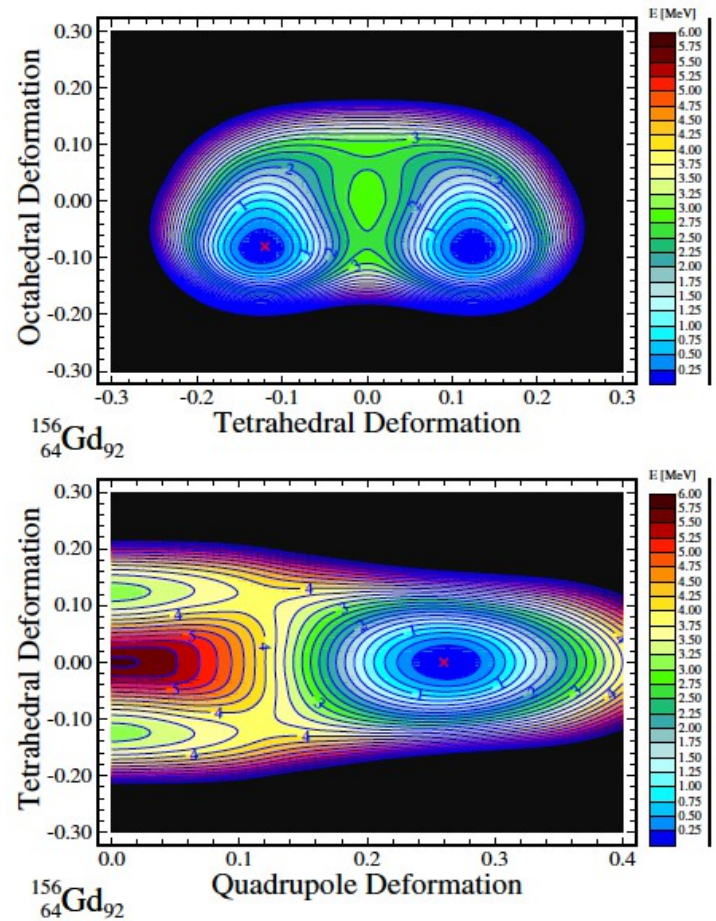

Disapperarance of γ-flatness in the Yb isotopes

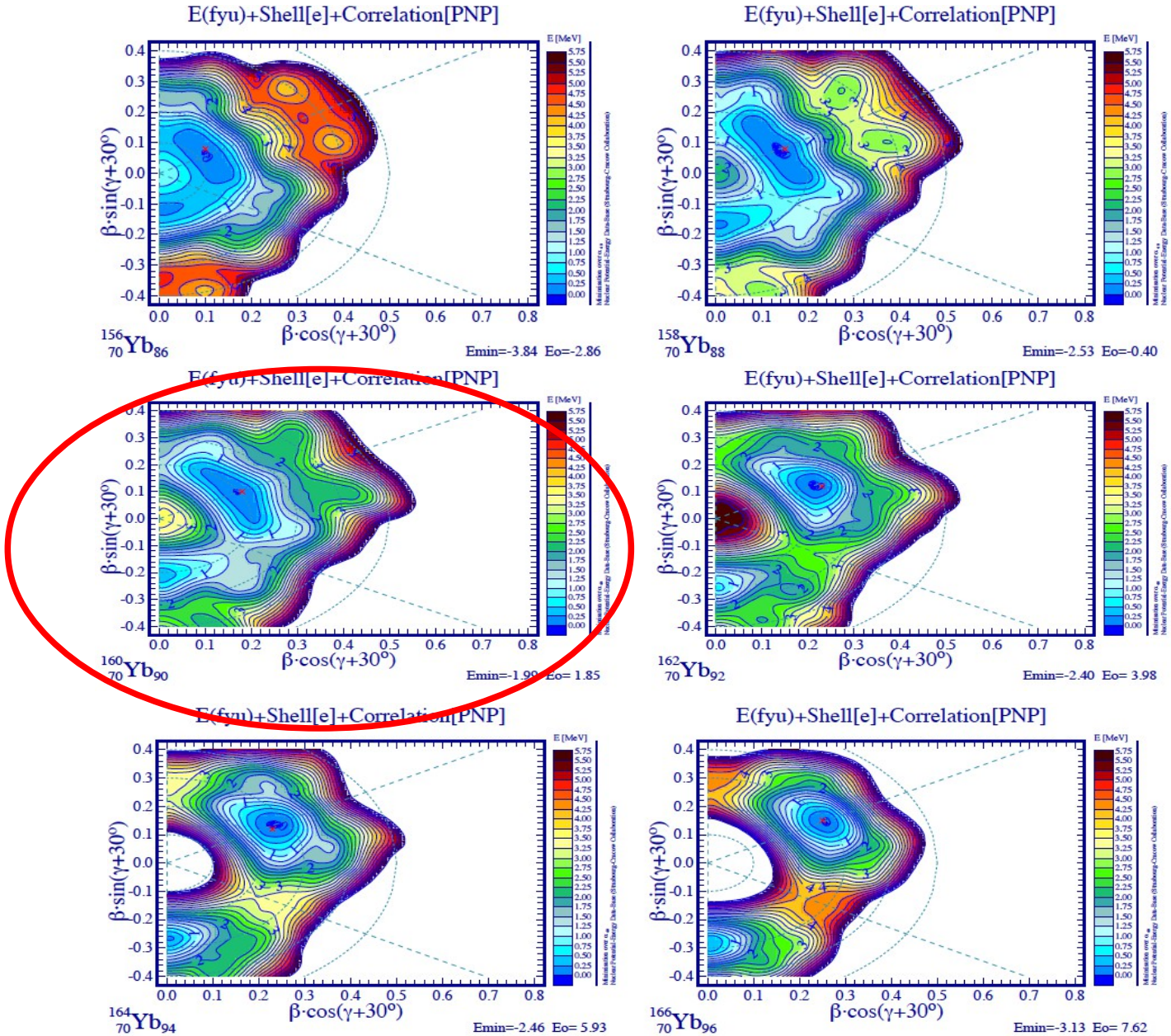

J. Dudek

Disapperarance of the α_{30} pear-shape octupole effects in the Yb isotopes

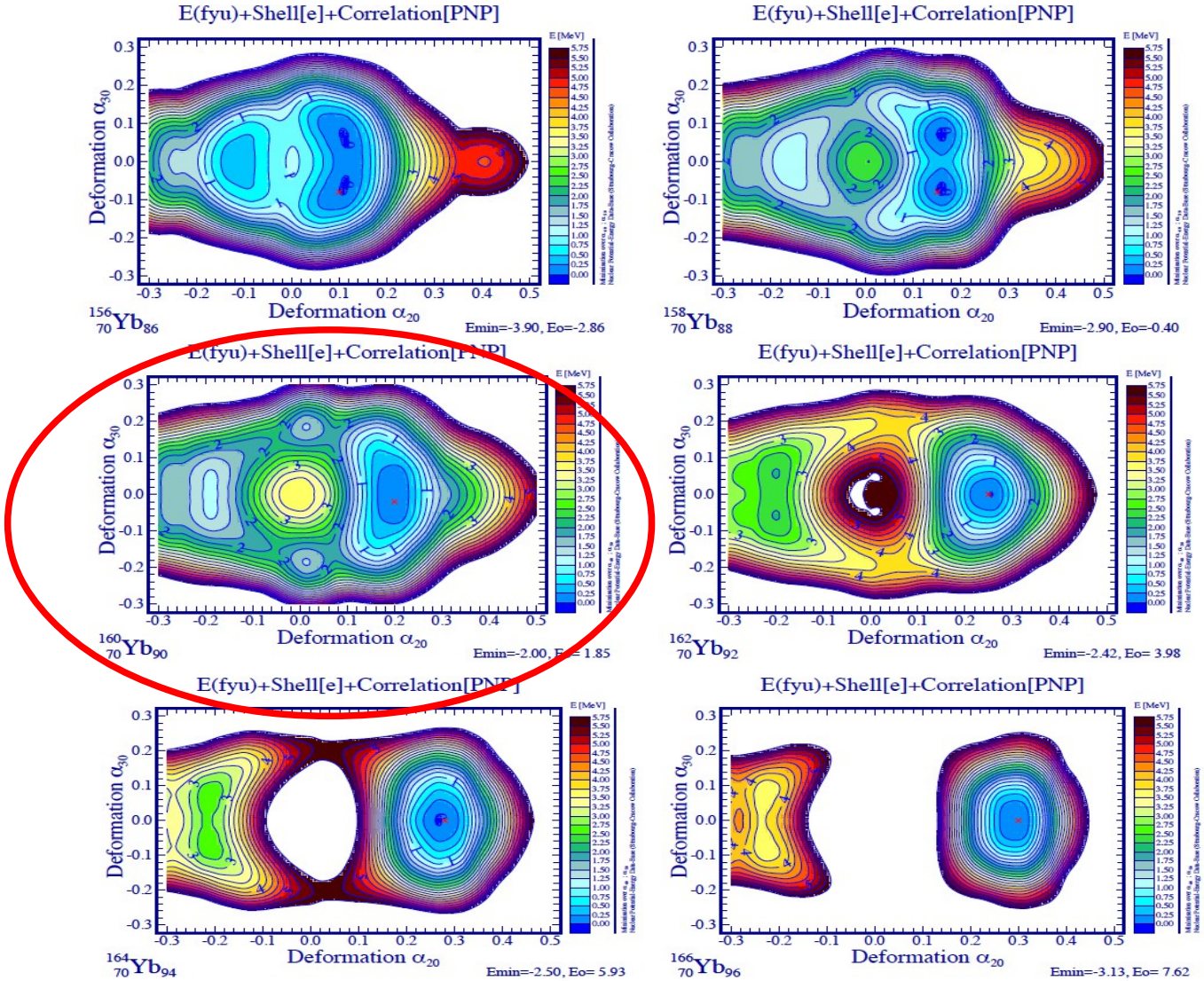

J. Dudek

Tetrahedral symmetry competition (the effect of α_{32}) and octupole effects in the Yb isotopes

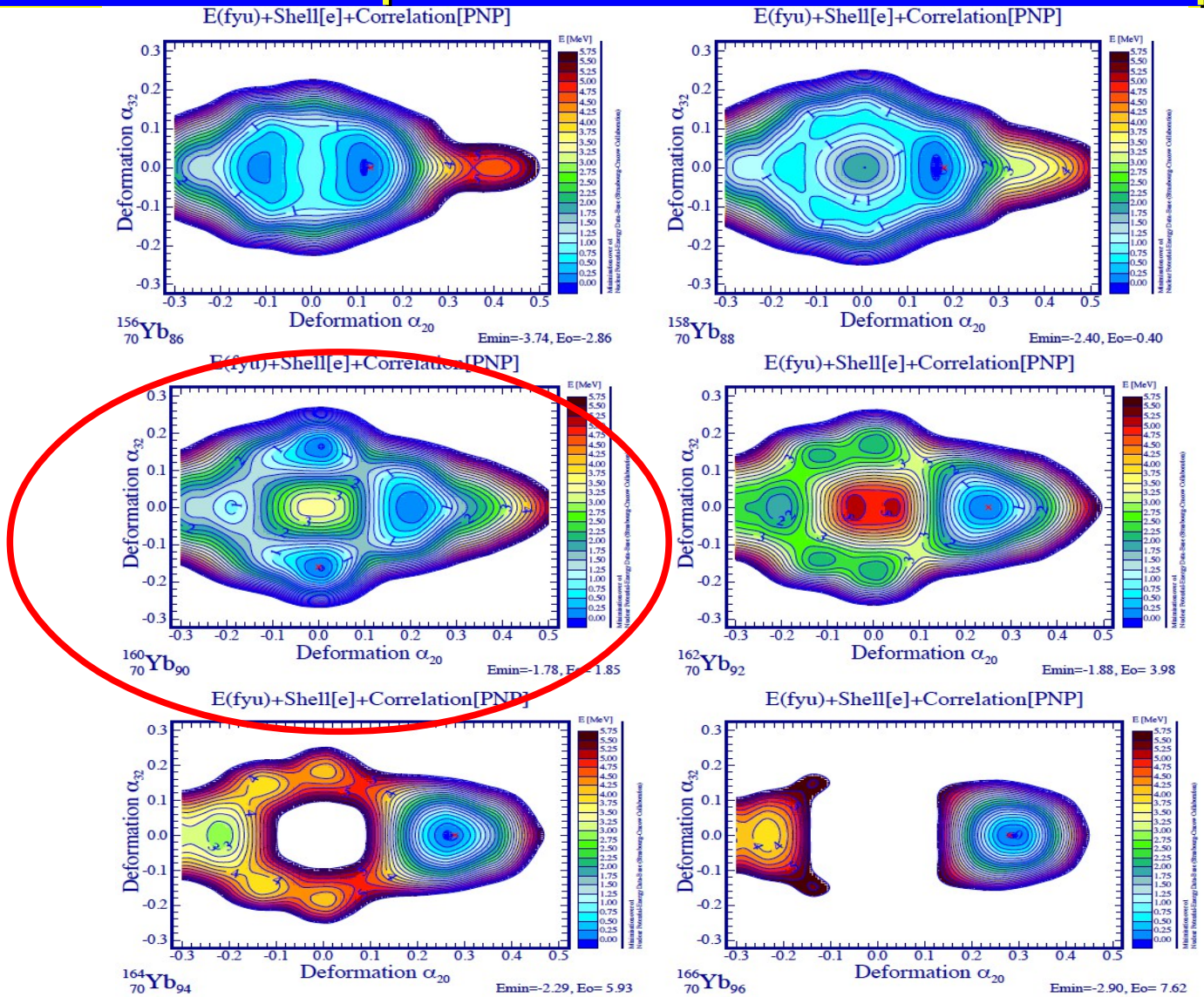

J. Dudek

Tetrahedral shape in ^{160}Yb ?

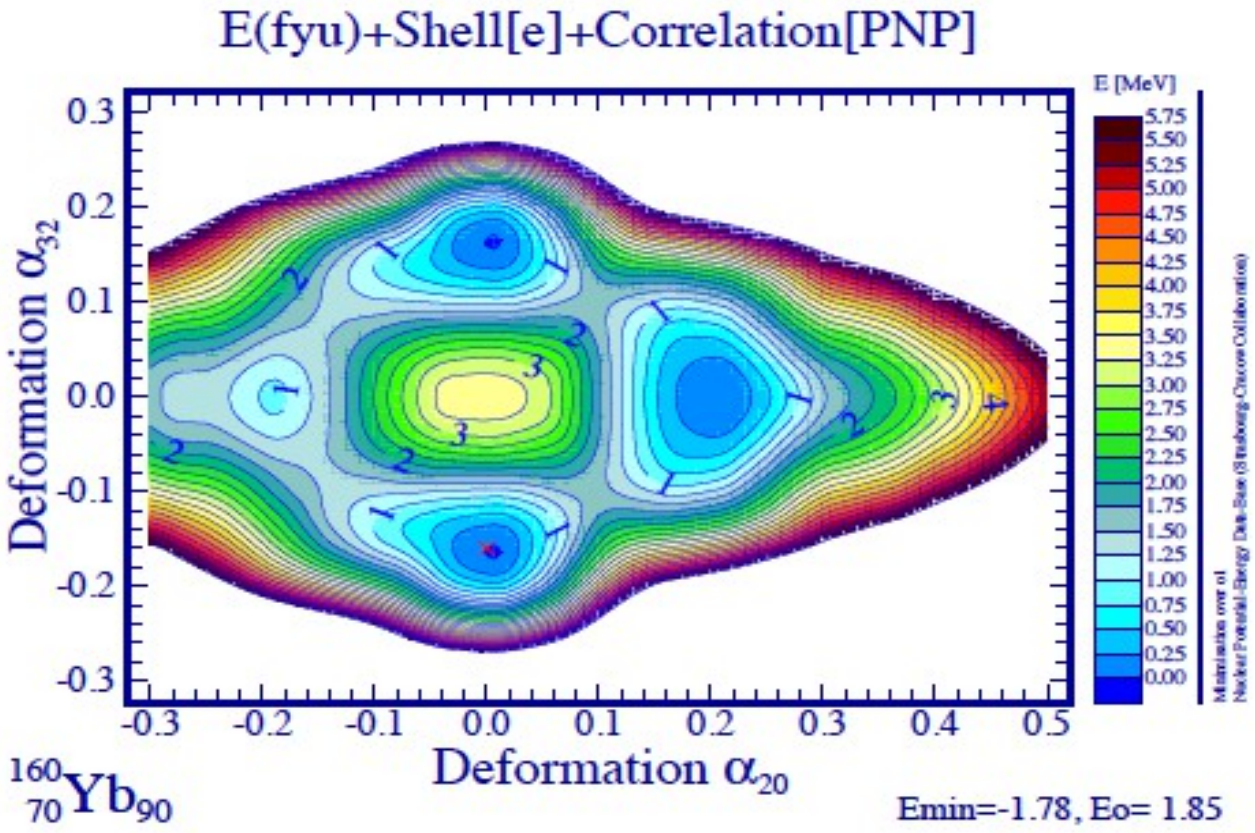

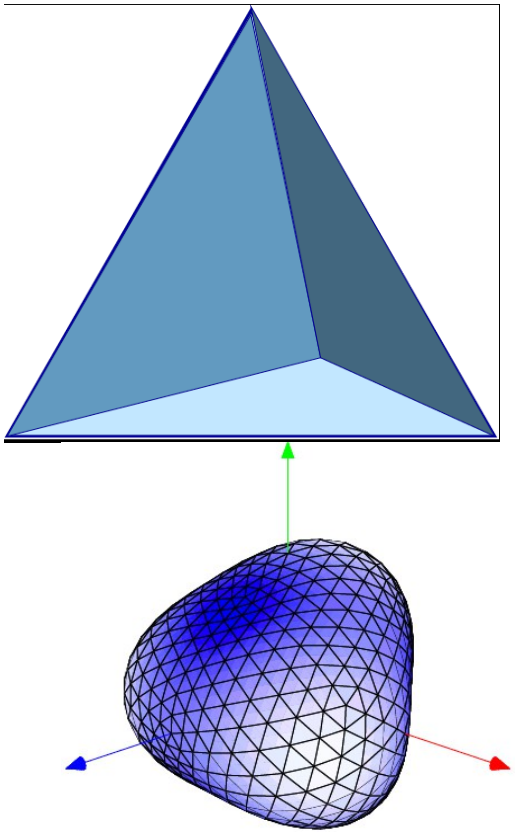

The ^{160}Yb case

β-decay

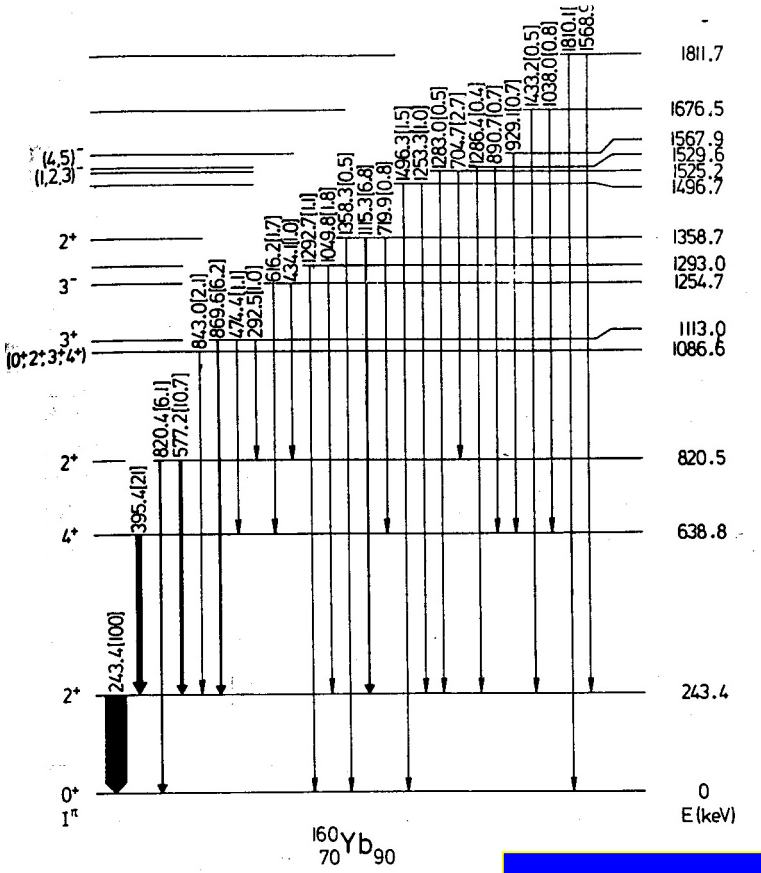

C. Garrett, PLB 118 (1982)

PRL 104, 022501 (2010) PHYSICAL REVIEW LETTERS week ending 15 JANUARY 2010

Nonzero Quadrupole Moments of Candidate Tetrahedral Bands

R. A. Bark,[1] J. F. Sharpey-Schafer,[2] S. M. Maliage,[1,2] T. E. Madiba,[1,2] F. S. Komati,[1,2] E. A. Lawrie,[1] J. J. Lawrie,[1] R. Lindsay,[2] P. Maine,[1,2] S. M. Mullins,[1] S. H. T. Murray,[1] N. J. Ncapayi,[1] T. M. Ramashidza,[1,2] F. D. Smit,[1] and P. Vymers[1,2]

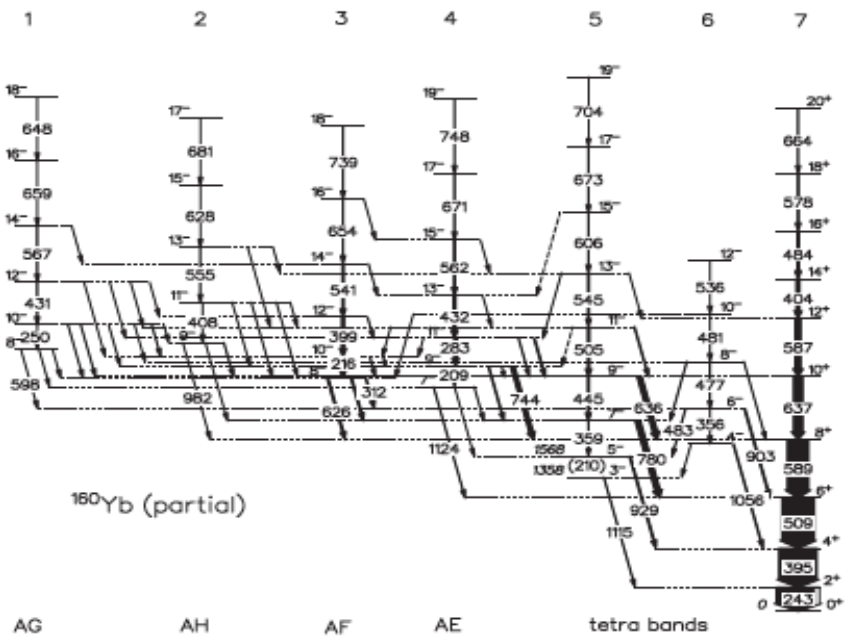

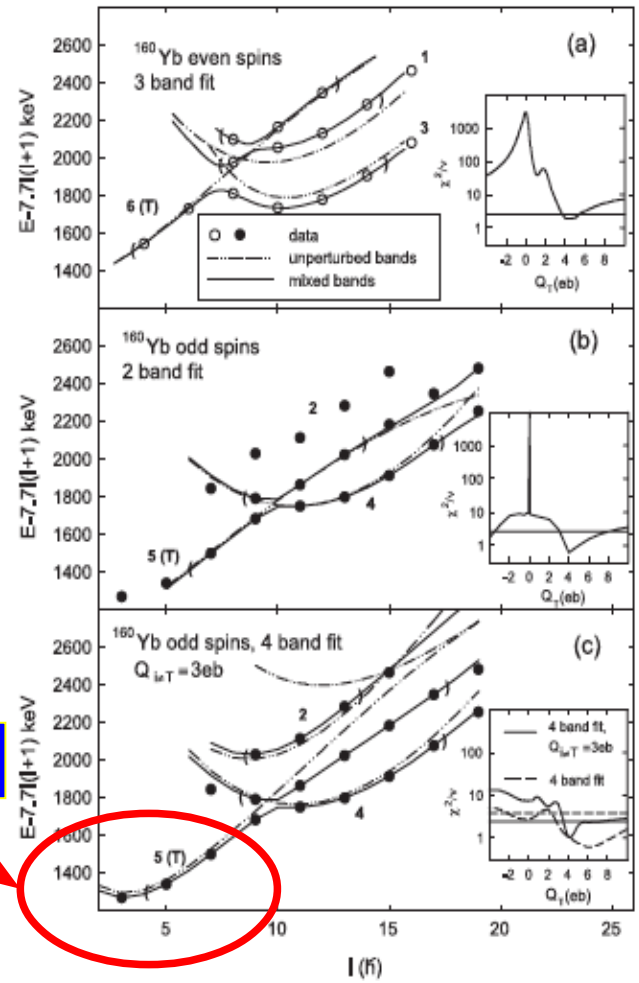

Coulex

The ^{160}Yb case

- The ^{160}Yb nucleus (Z=70 and N=90) is double-magic with respect to the predicted tetrahedral symmetry.
- The properties of the low-spin states, crucial to establish the symmetry, are not yet well known.
- The spin and parity assignments to a low-lying 1255 keV state are contradicting: 3^- or 4^+ ?
- The identification of the first 3^-, 5^-, 7^- states and their decay in-band and towards the ground-state band is crucial for the discovery of the tetrahedral bands.

The ^{160}Yb case

- To check if the populated negative-parity states are members of the tetrahedral band, one should measure with good accuracy the "feeding" transition probability B(E3)↑ and the de-excitation transition probabilities B(E3)↓, B(E2)↓ and B(E1)↓ knowing that the B(E2)/B(E1) branching ratios corresponding to the in-band to out-of-band are predicted 1÷2 orders of magnitude larger than in the standard octupole states.

Coulomb excitation

★Independent mechanism to preferentially populate collective non-yrast states.

★The 3^- states are normally non-yrast by ~1 MeV, and therefore one could question if they are efficiently populated in Coulomb excitation experiments.

★The answer is positive, as recently demonstrated in experiments of Coulomb excitation in inverse kinematics, in which the $3^- \rightarrow 2^+$ or the $3^- \rightarrow 4^+$ transitions of the stable Xe isotopes were seen at the level of 0.1% of the $2^+ \rightarrow 0^+$ transition.

GOSIA calculations for ^{160}Yb on ^{106}Pd and ^{197}Au

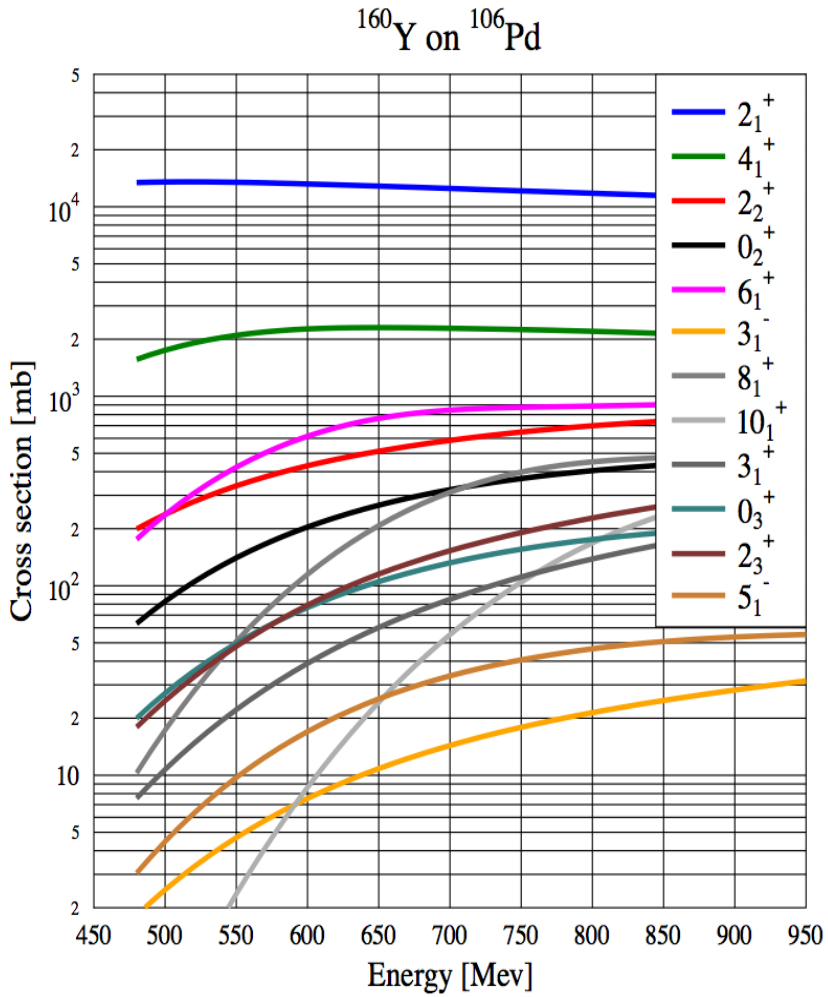

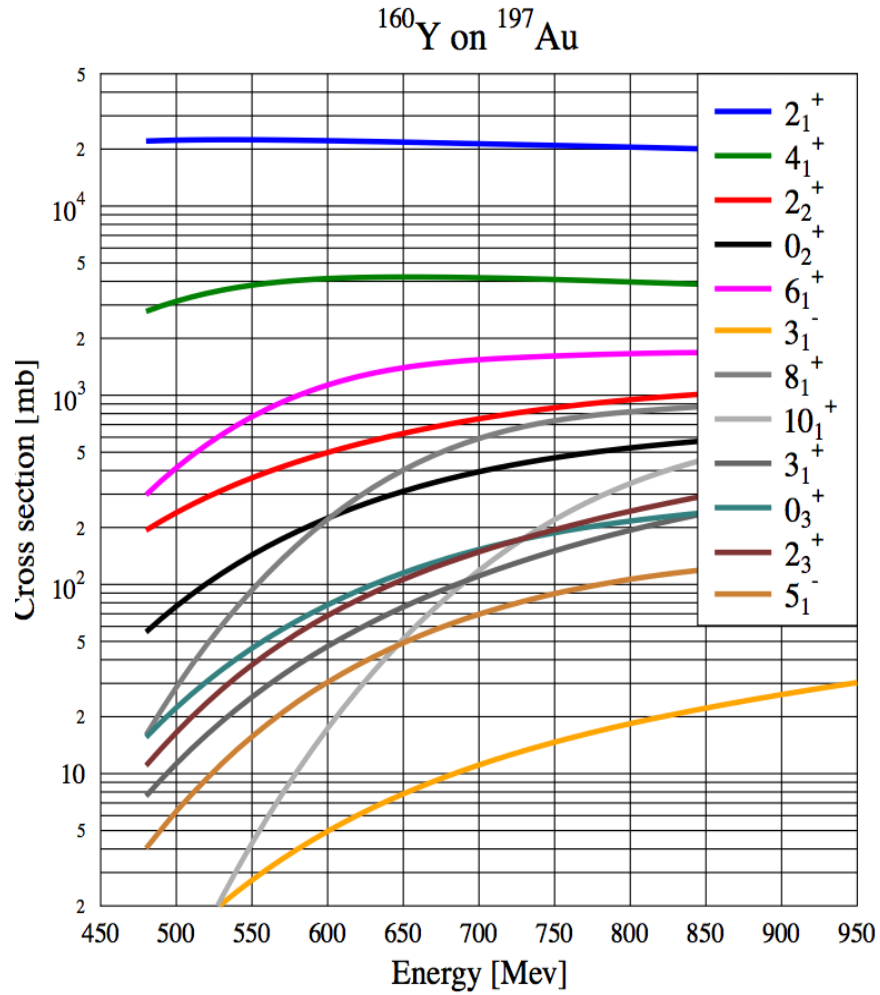

T. Konstantinopoulos

Critical point X(5) symmetry in N~90 nuclei

- The nuclei with N~90 (^{160}Yb,^{162}Yb,^{164}Yb) are the candidates in which the critical point symmetry X(5) is expected to be best realized.

Shape phase diagram in IBM

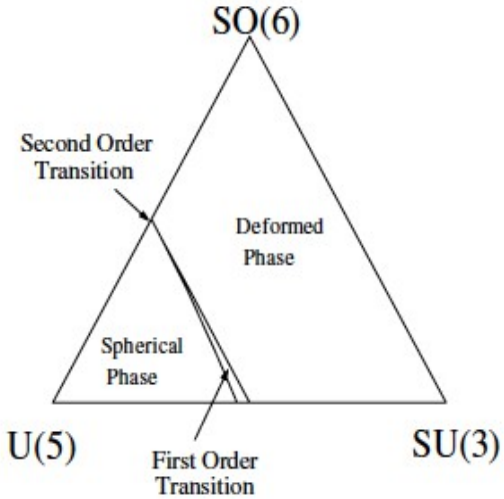

FIG. 2. Phase diagram of nuclei in the interacting boson model.

Iachello, Zamfir PRL 94 (2004)

Level scheme in X(5)

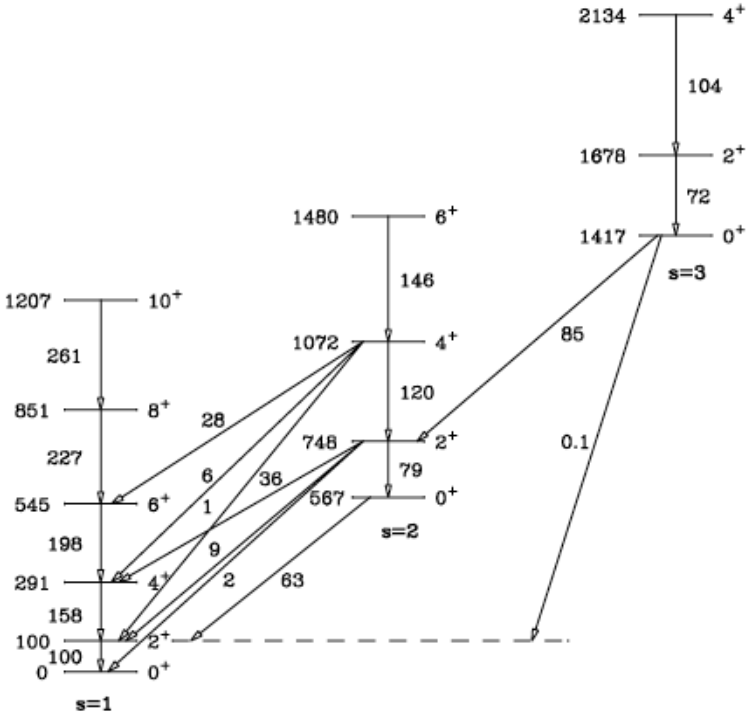

FIG. 2. Schematic representation of the lowest portion of the spectrum of X(5) symmetry. Only states with $n_\gamma = 0$ are shown. Energies are in units of the energy of the first excited state, $E_{2_1} - E_{0_1} = 100$. B(E2) values are in units of $B(E2; 2_{1_1} \rightarrow 0_{1_1}) = 100$.

Iachello, PRL 87 (2001)

Locus of the transition between spherical and deformed nuclei

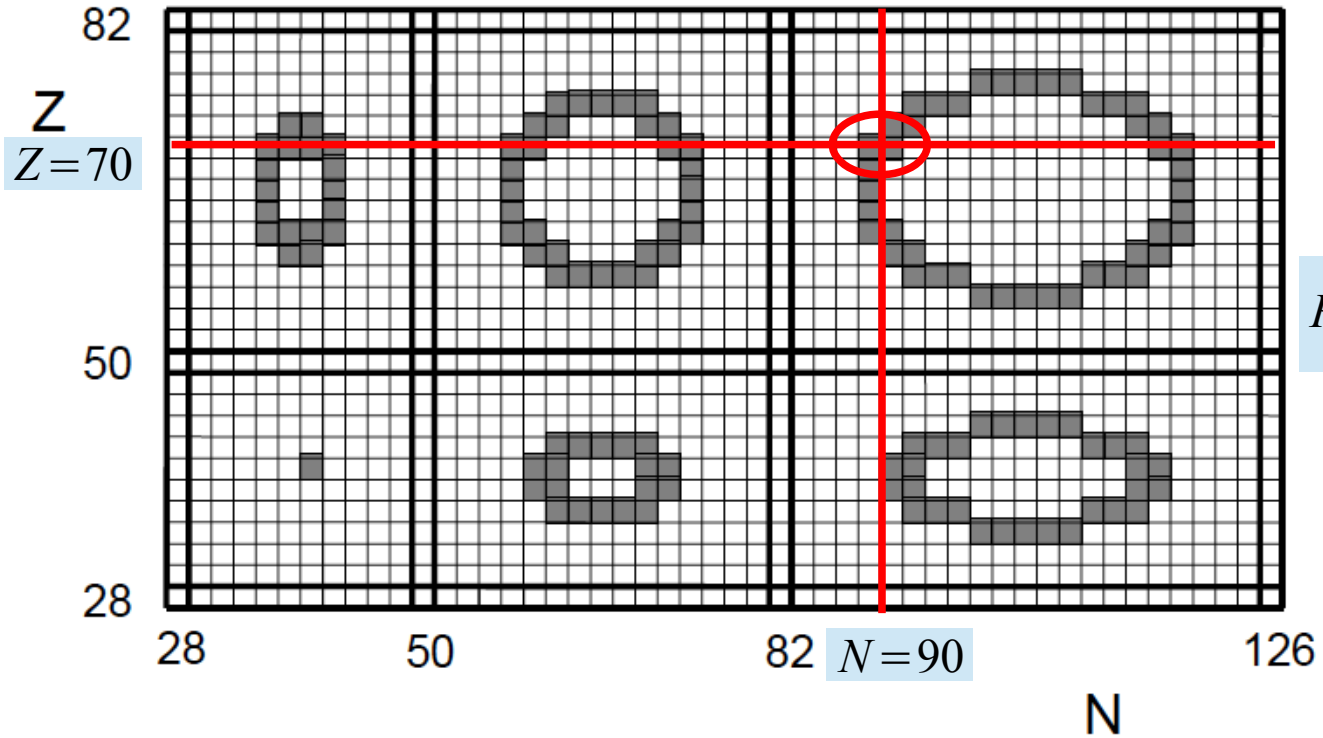

$$P=\frac{N_\pi N_\nu}{N_\pi+N_\nu}=5$$

Figure 3. Section of the nuclear chart in the N/Z plane. The shaded area gives the contours of P~5 values which give a guide to the locus of the transition between spherical and quadrupole deformed nuclei, i.e., the locus of potential X(5) critical point nuclei.

Critical point X(5) symmetry in Yb nuclei with N~90

78			2.30		2.26	2.44	2.51	2.70	2.68	2.56	2.53	2.49	2.48	2.48	Pt
76				2.62	2.66	2.74	2.93	3.02	3.09	3.15	3.20	3.17	3.08	2.93	Os
74		2.48	2.68	2.82	2.95	3.07	3.15	3.22	3.24	3.26	3.29	3.27	3.24	3.09	W
72	2.31	2.56	2.79	2.97	3.11	3.19	3.25	3.27	3.28	3.29	3.31	3.30	3.26		Hf
70	2.33	2.63	2.93	3.12	3.23	3.27	3.29	3.31	3.31	3.31					Yb
68	2.32	2.74	3.10	3.23	3.27	3.29	3.31	3.31	3.31						Er
66	2.23	2.93	3.21	3.27	3.29	3.30	3.31								Dy
64	2.19	3.01	3.24	3.29	3.30	3.30									Gd
62	2.32	3.01	3.25	3.29	3.30	3.30									Sm
60	2.49	2.93	3.27	3.29	3.32										Nd
58	2.59	2.86	3.15												Ce
56	2.66	2.84	2.99											$R_{4/2}$	Ba
Z/N	88	90	92	94	96	98	100	102	104	106	108	110	112	114	

$$P = \frac{N_\pi N_\nu}{N_\pi + N_\nu} = 5$$

^{160}Yb | ^{162}Yb

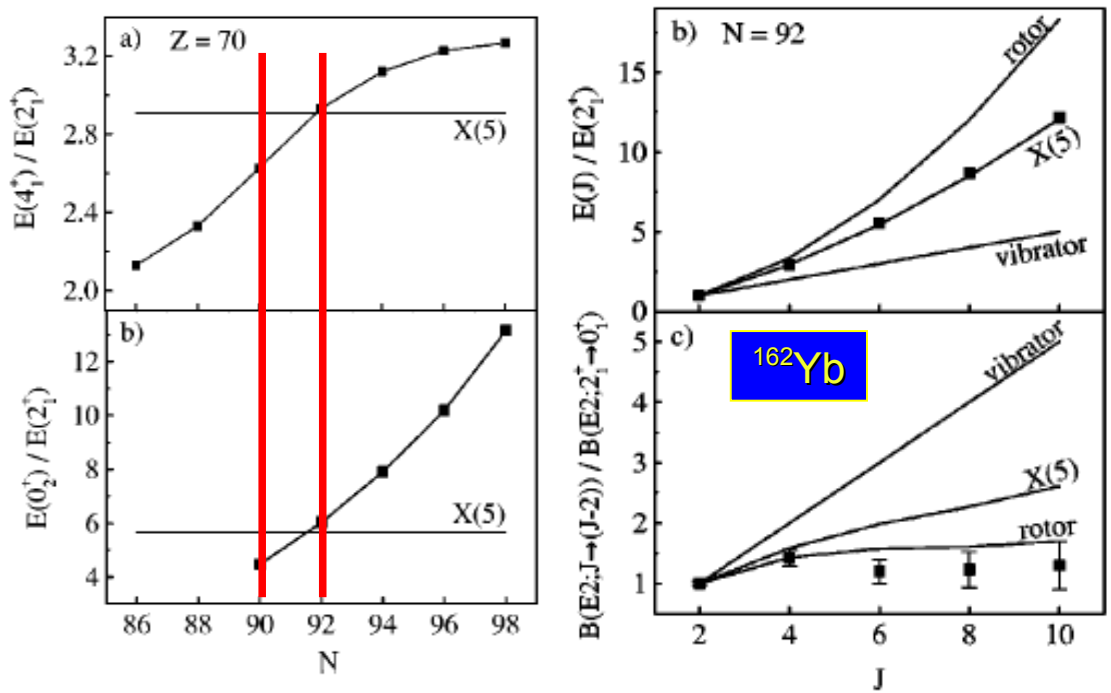

of ^{162}Yb relative to the X(5) critical point symmetry. If the currently accepted yrast $B(E2)$ values are verified, this nucleus, with the juxtaposition of a transitional $R_{4/2}$ value and rotational-like $B(E2)$ values, would be a challenge to microscopic theory.

McCutchan, PRC 69 (2004)

Transition between X(5) and rigid rotor

Deformation dependent models with different potentials: confined β-soft (CBS)

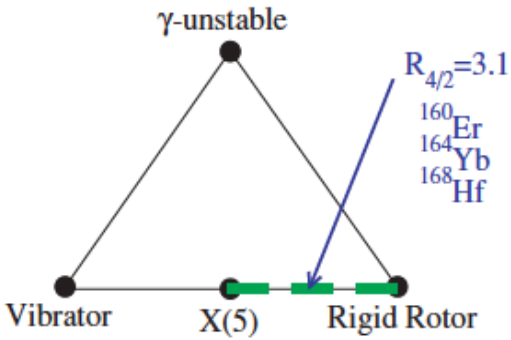

FIG. 1. (Color online) Schematic structural triangle for the nuclear collective model [9] where the vertices represent idealized limits of structure and the legs transition regions. The CBS model describes the transition region from X(5) to the symmetric rigid rotor (dashed line). Nuclides with $R_{4/2} = 3.1$ (e.g., ^{164}Yb, ^{168}Hf, and ^{160}Er, on which this paper focuses) might be intermediate between X(5) and the rigid rotor.

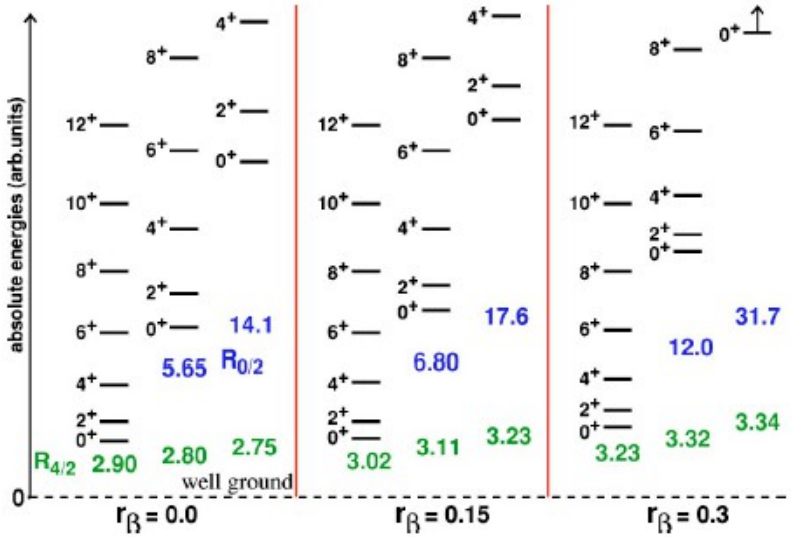

Pietralla, PRC 70 (2004); K. Dusling, PRC 73 (2006)

Davidson

$$u(\beta) = \beta^2 + \frac{\beta_0^4}{\beta^2},$$

PHYSICAL REVIEW C 76, 064312 (2007)

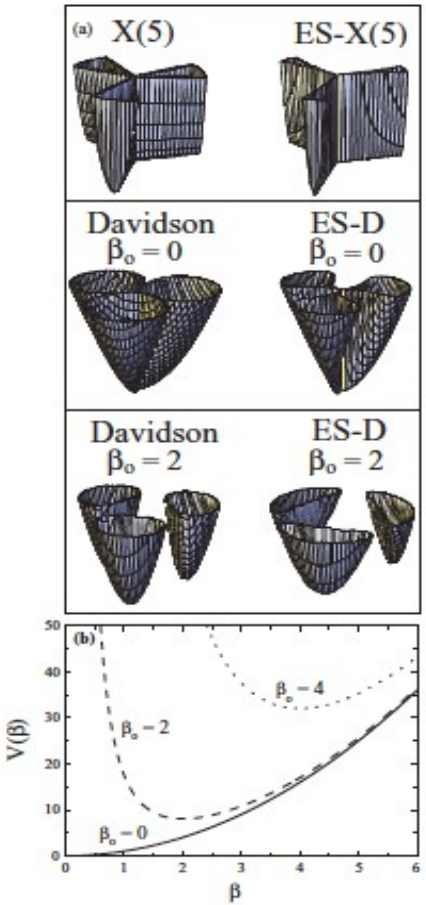

FIG. 1. (Color online) (a) Potentials in both the β and γ degrees of freedom for X(5) (top) and the Davidson potential with $\beta_0 = 0$ (middle) and $\beta_0 = 2$ (bottom). Potentials are shown for the approximate separation of variables (left) and the exact separation of the variables (right). (b) Davidson potential in the β degree of freedom for a few values of the parameter β_0.

Morse

$$u(\beta) = e^{-2a(\beta-\beta_e)} - 2e^{-a(\beta-\beta_e)}$$

PHYSICAL REVIEW C 77, 044302 (2008)

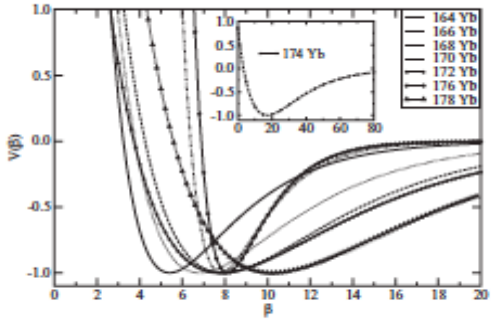

FIG. 2. Evolution of Morse potential shapes for the $_{70}$Yb isotopes, with the parameters given in Table II. See Sec. V for further discussion.

Kratzer

$$u(\beta) = -\frac{1}{\beta} + \frac{\tilde{B}}{\beta^2}$$

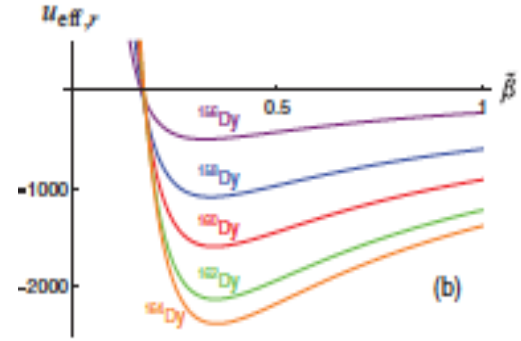

DENNIS BONATSOS *et al.*

PHYSICAL REVIEW C 88, 034316 (2013)

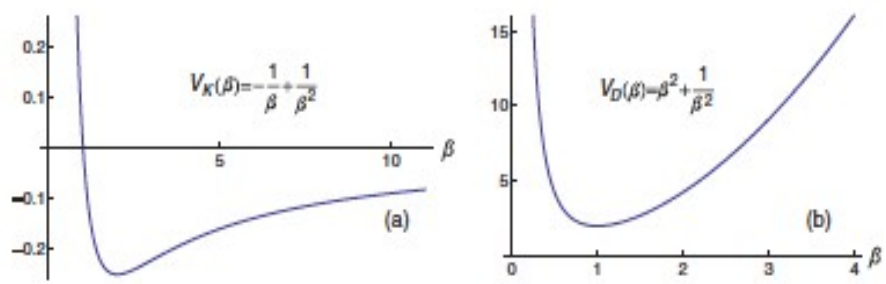

FIG. 1. (Color online) The Kratzer (left) and Davidson (right) potentials. The quantities shown are dimensionless, while all free parameters have been set equal to unity for the sake of simplicity.

D. Bonatsos

Thank you for your attention !